High-Resolution Range Profile Recognition Method of Vehicle Targets Based on Accelerated T-SNE with Multi-polarization Fusion

Hao Wu[1*], Dahai Dai[1], Penghui Ji[1], Bo Pang[1], Xuesong Wang[2]

[1.] State Key Laboratory of Complex Electromagnetic Environment Effects and Electronics and Information System, National University of Defense Technology, Changsha, China.

[2.] College of Electronic Science, National University of Defense Technology, Changsha, China.

jsczjtwh@126.com, ddh1206@163.com

2021 IEEE 6th International Conference on Signal and Image Processing (ICSIP) | 978-1-6654-3904-6/21/$31.00 ©2021 IEEE | DOI: 10.1109/ICSIP52628.2021.9688626

***Abstract*— Polarization plays an important role in analyzing radar targets. Full polarization information has a better ability to inverse fine structures of the target. However, previous studies of high-resolution range profile (HRRP) mainly neglected effects of polarization. Therefore, a novel radar target recognition algorithm based on accelerated t-Distributed Stochastic Neighbor Embedding(t-SNE) and multi-polarization weighted fusion has been proposed. Firstly, three single polarization channels, odd and even-bounce mechanism HRRP, and full polarization HRRP are described. The accelerated t-SNE method based on Barnes-Hut approximation improves the dimensionality reduction speed of processing HRRPs while maintaining the initial information of each HRRP. Also, it is capable of visualizing different targets. With the weighted fusion of posterior probabilities of multiple support vector machines (SVMs), we are able to realize recognition of targets. Experimental results of vehicle targets based on electromagnetic calculations show that recognition performance of this algorithm is superior to other methods, and it shows strong robustness under the condition of large azimuth angle.**

Keywords—multi-polarization fusion, polarimetric high resolution range profile, target visualization, target recognition

I. Introduction

Radar acquires target information by transmitting and receiving electromagnetic waves, so as to realize accurate target identification. Radar Targets can be roughly divided into two categories according to their generated attributes: natural targets and man-made targets. Research on natural targets is mainly concentrated in the field of remote sensing, while the application research on man-made targets such as ships and vehicles can not only bring convenience to civilian fields such as production and life, but also provide possibilities for precision guidance, tactical reconnaissance and the other military fields.

Great progress has been made in the field of vehicle target characteristics analysis and recognition. Wu. realized high-accuracy recognition with polarization scattering mechanism and scattering center theory based on the airspace and polarization scattering information within small azimuth angle classification [1]. A novel algorithm based on the circumscribed rectangle was proposed to accurately reflect the three-dimensional size information of the vehicle target in [2]. Fuller. proposed a multi-peak model, which effectively completed the modeling of the distributed attribute scattering center of vehicle targets [3]. Aiming at the problem of military vehicle target recognition, Ding. established a three-dimensional attribute scattering center model for target reconstruction and characterization [4]. Reference [5] discussed and researched on the characteristics analysis and recognition of vehicle targets under the condition of large-azimuth circular SAR imaging.

Polarization is an important attribute characteristic of electromagnetic waves. It represents the trajectory of the electric field vector in the cross section of the trajectory with time. In recent years, the research on analysis and recognition of radar polarization characteristics has attracted increasing amount of interest in radar community , which has effectively expanded the ability of target information extraction[6-7]. HRRP has been widely studied due to its simple formation principle, rich target information and multiple analysis methods[8-10]. Du et al. realized the recognition of three types of real-measured planes based on single-polarization power spectrum information[11]. Feng. used stacked autoencoders to build a deep neural network for identifying planes with HRRPs[12]. Xu et al. developed the ability of recurrent neural network and attention mechanism to extract the target area based on the sequence relationship of distance units in HRRP[13]. However, the vast majority of HRRP research in the past was limited to single-polarization conditions, and multi-polarization information has not been fully utilized. Therefore, it is very important to explore information fusion and target recognition under multi-polarization conditions.

This paper explores the fusion of HRRP under multi-polarization conditions, and enhances the analysis of polarization characteristics of HRRPs. On the basis of multi-polarization information fusion and maintaining the integrity of HRRP information, the dimension of HRRPs is reduced as much as possible. We are able to enhance the visualization ability of different civilian vehicle targets in two-dimensional and three-dimensional space, and improve the accuracy of target recognition.

This work has been supported in part by the National Natural Science Foundation of China (No. 61901499，No.61625108).

II. Polarization Theory and Formation of HRRPs

A. Polarization Theory

The horizontal and vertical polarization of polarized radar can be expressed by H and V respectively, and the polarization scattering matrix can be expressed by equation (1).

$$S=\begin{bmatrix} s_{HH} & s_{HV} \\ s_{VH} & s_{VV} \end{bmatrix} \tag{1}$$

Take s_{HV} as an example. The right side of the subscript represents the transmitting polarization, and the left side represents the reception polarization, that is, vertical polarization transmission and horizontal polarization reception. When the conditions of single station, far field and reciprocity are satisfied , the cross-polarization components are equal, i.e. $s_{HV}=s_{VH}$.

According to the definition of radar cross section (RCS), the relationship between scattering matrix elements and RCS is shown in the following equation.

$$\sigma_{pq}=4\pi\left|s_{pq}\right|^2 \qquad p,q=H,V \tag{2}$$

When fully polarized stepped frequency signal has been adopted for measurement without noise, the returned signal can be expressed as

$$\begin{aligned} r_{pq}(u)=\sum_{k=1}^{d} s_{k,pq}\exp\left(\frac{-j4\pi R_k f_0}{c}\right) \\ \bullet\exp\left(\frac{-j4\pi R_k(u-1)\Delta f}{c}\right) \end{aligned} \tag{3}$$

where $u=1,2,3,\cdots,U$, U is the total number of frequency points, c is the speed of light, f_0 represents initial frequency, Δf is frequency interval, R_k represents the distance between the k th scattering center and the radar. $s_{k,pq}$ is the scattering coefficient of the k th scattering center under pq polarization conditions. After inverse Fourier transform, HRRPs of the target can be obtained.

B. Multiple HRRP Forms

Suppose that the obtained i th group of HRRPs with pq polarization is expressed as $x_{i,pq}$

$$x_{i,pq}=\left[x_{i,pq}(1),x_{i,pq}(2),\cdots,x_{i,pq}(M)\right] \tag{4}$$

The mixture of HRRPs with three polarization in series can be obtained as

$$x_{i,all}=\begin{bmatrix} x_{i,HH} & x_{i,HV} & x_{i,VV}\end{bmatrix} \tag{5}$$

According to Pauli basis decomposition theory, HRRPs with odd-bounce scattering mechanism and HRRP with even-bounce scattering mechanism can be expressed as $x_{i,odd}$ and $x_{i,eve}$ respectively.

$$x_{i,odd}=\left(x_{i,HH}+x_{i,VV}\right)/2 \tag{6}$$

$$x_{i,eve}=\left(x_{i,HH}-x_{i,VV}\right)/2 \tag{7}$$

With different HRRPs under various scattering mechanisms, we can not only enhance the understanding of the size and structure of targets, but also provide more polarization information for subsequent target recognition.

III. Dimensionality Reduction of HRRP

In order to remove redundancy of HRRP and enhance visualization ability of targets, it is necessary to carry out dimensionality reduction operation on HRRP which helps realize low-dimensional visualization of different targets after dimensionality reduction processing. T-Distributed Stochastic Neighbor Embedding has the ability to preserve the local and global structure characteristics of data. With Barnes-Hut Approximation, we can speed up the processing of t-SNE[14-15].

A. t-SNE

The conditional probability of similarity between sample $x_{j,l}$ and sample $x_{i,l}$ is denoted as $p_{j|i,l}$,

$$p_{j|i,l}=\begin{cases} \dfrac{\exp\left(-\left\|x_{i,l}-x_{j,l}\right\|^2/2\sigma_{i,l}^2\right)}{\sum_{k\neq i}\exp\left(-\left\|x_{i,l}-x_{k,l}\right\|^2/2\sigma_{i,l}^2\right)}, & i\neq j \\ 0, & i=j \end{cases} \tag{8}$$

where l is the type of targets and $\sigma_{i,l}$ is the gaussian variance of $x_{i,l}$.

The joint probability of two HRRP samples defined in t-SNE can be expressed as $p_{ij,l}$ and N represents the total number of HRRPs

$$p_{ij,l}=\frac{p_{i|j,l}+p_{j|i,l}}{2N} \tag{9}$$

We define the joint probability $q_{ij,l}$ to describe the similarity of the corresponding HRRPs $y_{j,l}$ and $y_{i,l}$ after dimensionality reduction.

$$q_{ij,l}=\begin{cases} \dfrac{\left(1+\left\|y_{i,l}-y_{j,l}\right\|^2\right)^{-1}}{\sum_{k\neq g}\left(1+\left\|y_{k,l}-y_{g,l}\right\|^2\right)^{-1}}, & i\neq j \\ 0, & i=j \end{cases} \tag{10}$$

The HRRPs $y_{j,l}$ and $y_{i,l}$ after dimensionality reduction should be similar to HRRPs $x_{j,l}$ and $x_{i,l}$ .Therefore, KL divergence C_l that minimizes the joint probability distribution of two spaces is constructed to determine the HRRPs after dimensionality reduction.

$$C_l = KL\left(P_l \| Q_l\right) = \sum_{i \neq j} p_{ij,l} \log \frac{p_{ij,l}}{q_{ij,l}} \tag{11}$$

We usually use gradient descent method to solve the above formula.

B. Accelerated t-SNE

The gradient of C_l can be expressed as

$$\frac{\delta C_l}{\delta y_i} = 4\sum_{j \neq i}\left(p_{ij,l} - q_{ij,l}\right) q_{ij,l}\left(y_{i,l} - y_{j,l}\right) Z_l \tag{12}$$

where $Z_l = \sum_{k \neq g}\left(1 + \left\| y_{k,l} - y_{g,l} \right\|^2\right)^{-1}$.

The above formula can be transformed into

$$\begin{aligned} \frac{\delta C_l}{\delta y_i} &= 4\left(F_1 + F_2\right) \\ &= 4\sum_{j \neq i} p_{ij,l} q_{ij,l}\left(y_{i,l} - y_{j,l}\right) Z_l \\ &\quad - 4\sum_{j \neq i} q_{ij,l} q_{ij,l}\left(y_{i,l} - y_{j,l}\right) Z_l \end{aligned} \tag{13}$$

We approximate F_2 more effectively by adopting a quadtree or octree in Barnes-Hut approximation, so as to improve the computational efficiency while losing less precision.

IV. Multi-classifier Fusion Processing

For a polarization HRRP of an unknown category, after the dimensionality reduction visualization operation, we use the previously trained support vector machines to obtain the posterior probability p_{ij} of the polarization HRRPs that belongs to different categories[16]. Where $i = 1, 2, \cdots, N$ and $j = 1, 2, \cdots, M$, the posterior probability output matrix is expressed as P_{pos}

$$P_{pos} = \begin{bmatrix} p_{11}(F_1) & p_{12}(F_1) & p_{13}(F_1) & \cdots & p_{1M}(F_1) \\ p_{21}(F_2) & p_{22}(F_2) & p_{23}(F_2) & \cdots & p_{2M}(F_2) \\ p_{31}(F_3) & p_{32}(F_3) & p_{33}(F_3) & \cdots & p_{3M}(F_3) \\ \vdots & \vdots & \vdots & \ddots & \vdots \\ p_{N1}(F_N) & p_{N2}(F_N) & p_{N3}(F_N) & \cdots & p_{NM}(F_N) \end{bmatrix}_{N \times M} \tag{14}$$

The i th row in P_{pos} represents the posterior probability of the i th SVM classifier SVM_i when the input feature is F_i after dimensionality reduction, and the maximum probability column indicates the predicted category of the sample.

We calculate the Shannon entropy $H_i(F_i)$ that characterizes the classification ability of different support vector machines SVM_i for the specific feature F_i .

$$H_i(F_i) = -\sum_{j=1}^{M} p_{ij} \log_2 p_{ij},\ i = 1, 2, 3, \cdots, N \tag{15}$$

The weights w_i of different support vector machines SVM_i is denoted as

$$w_i = \frac{\exp\left(-H_i(F_i)\right)}{\sum_{j=1}^{N} \exp\left(-H_i(F_i)\right)}, i = 1, 2, 3, \cdots, N \tag{16}$$

Then the posterior probability of each feature is weighted and summed up, and we can obtain P_{vot}

$$P_{vot} = \left[\sum_{i=1}^{N} w_i p_{i1}, \sum_{i=1}^{N} w_i p_{i2}, \sum_{i=1}^{N} w_i p_{i3}, \cdots, \sum_{i=1}^{N} w_i p_{iM}\right] \tag{17}$$

The column corresponding to the maximum value in P_{vot} is the predicted category, so that we can realize fusion and recognition of the corresponding civilian vehicle target with multi-polarization HRRPs.

$$Class = \arg\max_j \left\{\sum_{i=1}^{N} w_i p_{ij}\right\}, j = 1, 2, 3, \cdots, M \tag{18}$$

V. Experiments and Discussions

The electromagnetic dataset of vehicle targets used in this paper was released by the U.S. Air Force Research Laboratory and the Ohio State University[17].

TABLE I. ELECTROMAGNETIC CALCULATION PARAMETERS

Radar Parameter	Value
Radar center frequency	9.6GHz
Bandwidth	5.35GHz
Frequency points	512
Azimuth angle range	360°
Azimuth angle interval	0.0625°
Maximum unambiguous range	14.314m
Polarization mode	HH，HV，VV

As shown in TABLE 1, vehicle electromagnetic calculation data parameters are displayed. The radar center frequency is 9.6GHz, the radar bandwidth is 5.35GHz, and the number of frequency points is 512. Also the azimuth angle range is 360°, corresponding azimuth angle interval is 0.0625°, and the maximum unambiguous distance is 14.314m. The pitch angle adopted in this paper is 30°.

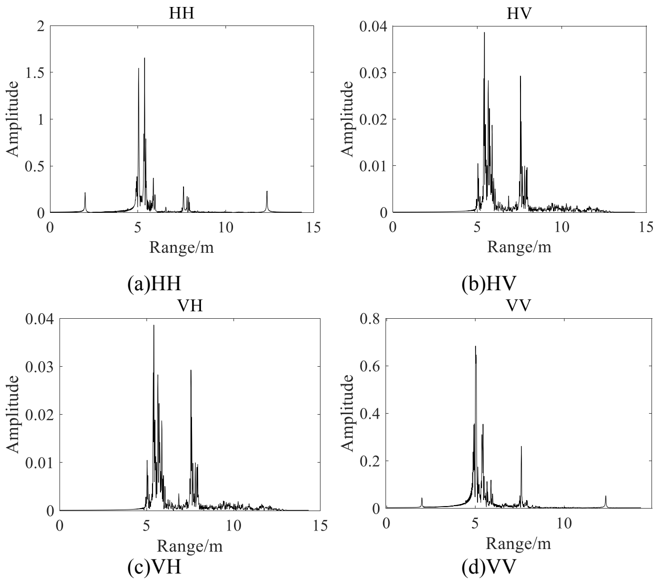

(a)HH (b)HV

(c)VH (d)VV

Fig. 1. HH,HV,VH and VV polarization HRRP of Mitsubishi when the azimuth angle is 0

Fig. 1 shows the full polarization HRRP of Mitsubishi when the azimuth angle is 0. Considering the assumption that there is reciprocity between HV and VH polarization channels, the HRRPs of HV and VH polarization are the same. When the azimuth angle is 0, the energy of HRRP of HH polarization is generally greater than that of VV polarization, and the energy obtained by co-polarization HRRP is much greater than that of cross-polarization.

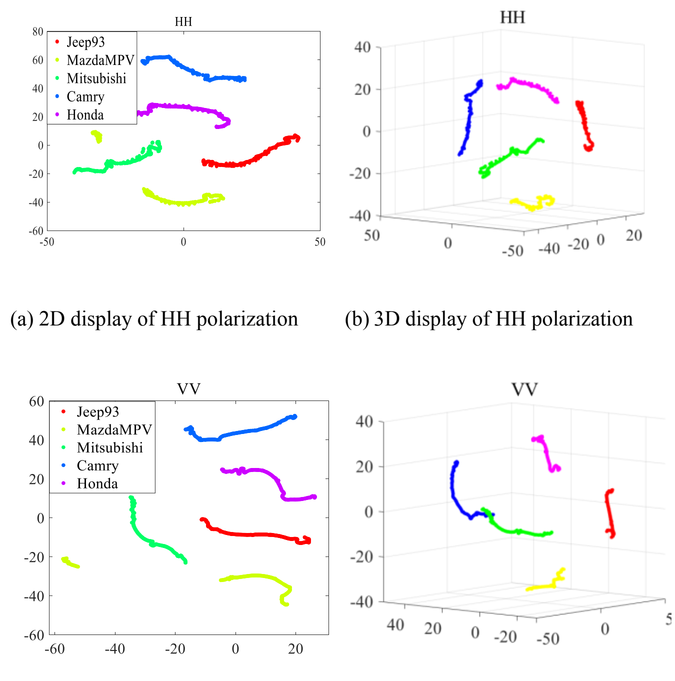

(a) 2D display of HH polarization (b) 3D display of HH polarization

(c) 2D display of VV polarization (d) 3D display of VV polarization

Fig. 2. Multi-dimensional space display of five civilian vehicle targets with HH and VV polarization after HRRP dimensionality reduction.

Fig.2 (a) and (c) show the 2D display of 500 HRRP samples with HH and VV polarization after dimensionality reduction, which contains five kinds of vehicles, the sample number of each kind is 100. The red dot represents Jeep93, the yellow dot represents MazdaMPV, the green dot represents Mitsubishi, the blue dot represents Camry, and the purple dot represents Honda. After the dimensionality reduction of the five vehicles, the data points can be better separated in 2D space, and points represent the same target exhibit a good aggregation effect, while sufficient distance between different target groups is maintained. Fig. 2(b) and (d) displays 500 HRRP samples in 3D space of the five types of vehicles with HH and VV polarization. The points represented by the five types of vehicles can also be effectively separated in 3D space. Due to the dimension has been extended to three, the separation ability between different targets has been enhanced.

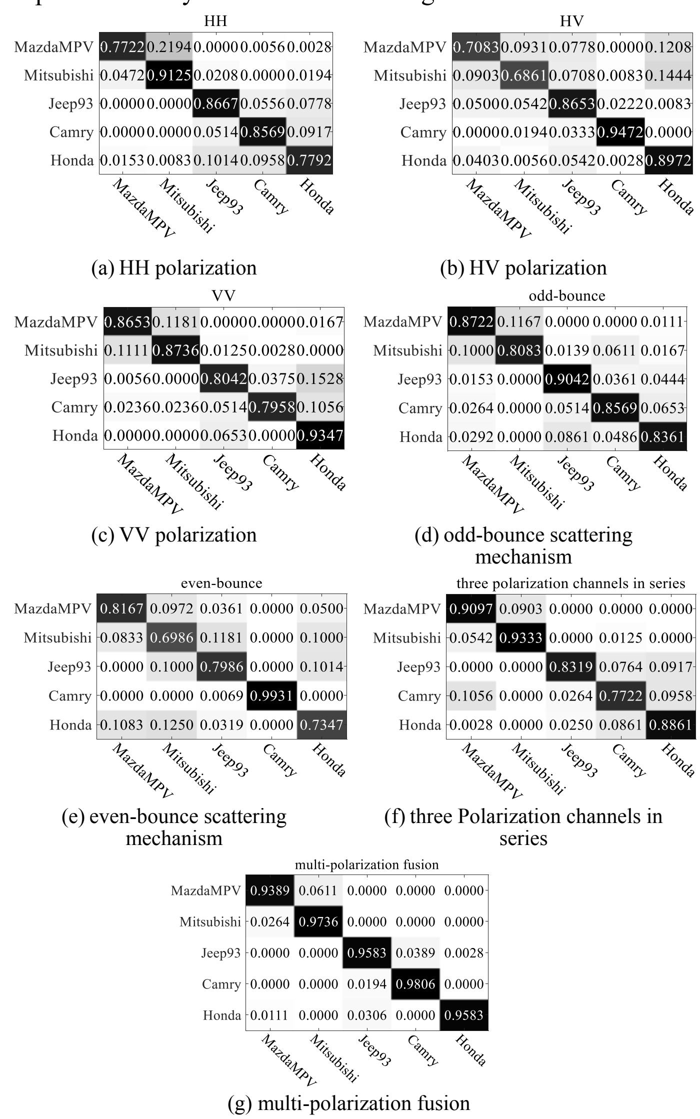

(a) HH polarization (b) HV polarization

(c) VV polarization (d) odd-bounce scattering mechanism

(e) even-bounce scattering mechanism (f) three Polarization channels in series

(g) multi-polarization fusion

Fig. 3. Comparison of classification results of three single polarization channels, odd-bounce and even-bounce scattering mechanism,three polarization channels in series and multi-polarization fusion HRRP

Fig. 3 shows the recognition results of three single polarization channels, odd-bounce and even-bounce scattering mechanism, three polarization channels in series and multi-polarization fusion HRRP. The azimuth angle range of HRRPs adopted in Fig. 3 is 90°, the number of samples is 1440, 50% of the samples are randomly selected for training, and the remaining 50% samples are for testing. The classification accuracy of vehicle targets obtained by adopting three single-polarization HRRPs of HH, HV and VV is mostly less than 90%, and the average classification accuracy with single polarization is less than 86%. With odd-bounce scattering mechanism, the classification accuracy of each vehicle is higher than 80%, however, the highest classification accuracy is lower than 91%. The recognition accuracy of the Mitsubishi can only reach 69.86% with even-scattering mechanism. The recognition rate of HRRPs obtained by using three polarization channels in series is more stable than that of single polarization channel. With multi-polarization fusion HRRPs, the recognition rate of five types of vehicles has been greatly improved. The recognition rate of all targets has reached more than 94.5%, which is superior to the other six HRRP forms.

VI. Conclusion

This paper has proposed a novel radar target recognition algorithm that integrates six different HRRP forms with multi-polarization fusion. In this paper, the speed of HRRP dimensionality reduction has been improved, and the low-dimensional data obtained by the weighted support vector machines has been adopted. We fuse the obtained low-dimensional data from six forms of HRRPs to realize more accurate recognition of civilian vehicles.

Acknowledgment

We would like to thank the U.S. Air Force Research Laboratory and the Ohio State University for sharing the electromagnetic dataset of civilian vehicles.

References

[1] J.Wu, Y.Chen, D.Dai, B.Pang, X. Wang. “Scattering mechanism identification based on polarimetric HRRP of manmade target,”. Journal of Radars, vol. 5(2), pp. 174–181,2016.

[2] H.Wu. “Polarization Feature Extraction of Artifical Target and Inversion of Meticulous Geometry Structure,” Changsha: National University of Defense Technology, 2017.

[3] D.F.Fuller, M.A.Saville. “A High-Frequency Multipeak Model for Wide-Angle SAR Imagery,” IEEE Transactions on Geoscience and Remote Sensing, vol. 51(7),pp. 4279-4291,2013.

[4] B. Ding, G. Wen. “Target Reconstruction Based on 3-D Scattering Center Model for Robust SAR ATR,” IEEE Transactions on Geoscience and Remote Sensing, vol. 56(7),pp.3772-3785,2018.

[5] M.A.Saville, J.A. Jackson, D. F. Fuller. “Rethinking vehicle classification with wide-angle polarimetric SAR,” IEEE Aerospace and Electronic Systems Magazine, vol. 29(1),pp.41-49 ,2014.

[6] H.Wu, D.Dai, X.Wang. “A Novel Radar HRRP Recognition Method with Accelerated T-Distributed Stochastic Neighbor Embedding and Density-Based Clustering,” Sensors,vol.19(23), 5112, 2019.

[7] H.Wu, P.Pang. “Unmanned Aerial Vehicle Recognition Based on Clustering by Fast Search and Find of Density Peaks (CFSFDP) with Polarimetric Decomposition,” Electronics, vol.7(12), 364,2018.

[8] C. Mao, J. Liang. “HRRP Recognition in Radar Sensor Network,” Ad Hoc Networks, vol.58,pp.171-178,2017.

[9] F. Zhao, Y. Liu, K. Huo, et al. “Radar HRRP Target Recognition Based on Stacked Autoencoder and Extreme Learning Machine,” Sensors, vol. 18(1),pp.173,2018.

[10] D.Zhou. “Radar target HRRP recognition based on reconstructive and discriminative dictionary learning,”Signal Processing,vol.126(9), pp.52-64,2016.

[11] L.Du, H.Liu, Z.Bao, et al. “Radar HRRP target recognition based on higher order spectra,” IEEE Transactions on Signal Processing,vol. 53(7), pp.2359-2368,2005.

[12] B.Feng, B.Chen, H.Liu. “Radar HRRP target recognition with deep networks,” Pattern Recognition, vol. 61, pp.379-393,2017.

[13] B. Xu, B. Chen, J. Wan, et al. “Target-aware recurrent attentional network for radar HRRP target recognition,” Signal Processing,vol. 155, pp. 268-280, 2019.

[14] V. D. M. Laurens. “Accelerating t-SNE using tree-based algorithms,” JMLR.org, 2014.

[15] V. D. M. Laurens, G. Hinton. “Visualizing Data using t-SNE,” Journal of Machine Learning Research, vol.9(2605), pp.2579-2605, 2008.

[16] W. Chen. “Research on Radar HRRP Target Recognition Technology Based on Feature Extraction,” Nanjing University of Aeronautics and Astronautics,2018.

[17] K. E. Dungan, C. Austin, J. Nehrbass, C. L. Potter. “Civilian vehicle radar data domes,” Proceedings of SPIE, 7699,2010.